

Position displacement of diffuse interstellar bands ¹

G. Galazutdinov^{1,2}

¹ *Instituto de Astronomia, Universidad Catolica del Norte, Av. Angamos 0610, Antofagasta, Chile*

² *Pulkovo Observatory, Pulkovskoe Shosse 65, Saint-Petersburg 196140, Russia*

runizag@gmail.com

J. Krelowski

Center for Astronomy, Nicholas Copernicus University, Gagarina 11, Pl-87-100 Toruń, Poland

jacek@astri.uni.torun.pl

Y.Beletsky

Las Campanas Observatory, Carnegie Observatories, Casilla 601, La Serena, Chile

ybelets@gmail.com

and

G.Valyavin

Special Astrophysical Observatory, Nizhnij Arkhyz, Russia

gvalyavin@gmail.com

ABSTRACT

We re-consider the already published phenomenon: the blue shift of diffuse interstellar bands, observed in spectra of HD34078 (AE Aur) and members of the Sco OB1 association, in particular HD152233. We have analyzed 29 diffuse bands. Part of them, already proven as blue-shifted in our earlier study, are now confirmed using another instrument: this time the 6.5m Clay telescope equipped with the MIKE spectrograph. The high signal-to-noise ratio (over 600) of our spectra allowed us to reveal even small scale **displacements** of positions (both: blue and red-shifts) of diffuse bands along the considered lines of sight. In some cases the magnitude of deviation exceeds 10 km s^{-1} . Also, we prove that profiles of many diffuse bands in spectra of HD34078 suffer significant broadening. The origin of the observed phenomena is discussed.

Subject headings: ISM: lines and bands

¹This paper includes data gathered with the 6.5 meter Magellan Telescopes located at Las Campanas Observatory(Chile).

1. Introduction

Diffuse interstellar bands (DIBs) have been known since the discovery by Heger in 1922 recalled recently in a nice form by McCall and Griffin (2013). After more than 90 years they remain unidentified; the identity of their carriers is thus the longest standing unanswered question in all of spectroscopy. The current list of unidentified interstellar absorption features, observable in translucent interstellar clouds, contains more than 400 entries (Hobbs et al., 2008, 2009). Despite many laboratory based studies of possible DIB carriers, it has not been possible to unambiguously link these bands to specific species. This is unfortunate, as an identification of DIBs would substantially contribute to our understanding of chemical processes in the diffuse interstellar medium. The presence of substructures inside DIB profiles, discovered by Sarre et al. (1995) and by Kerr et al. (1998), supports the idea that DIBs are very likely molecular features of numerous carriers that remain in the gas phase in interstellar translucent clouds.

Establishing the rest wavelengths of DIBs is not a trivial task as they have never been observed in laboratories. The only way to accomplish this job is to move the whole spectrum to the rest wavelength velocity frame using identified interstellar atomic or molecular lines. The existing surveys display slightly different central wavelengths for the same DIBs (Tab. 1); this is natural since the DIB profiles are nonsymmetric and thus the measurements of their wavelengths depend on the chosen central points. Moreover, in some cases DIB profiles are likely suffering the Doppler split (Herbig & Soderblom 1982; Weselak et al. 2010) which makes the task of determining central wavelengths even more complicated. To avoid uncertainties introduced by these problems we have selected targets without an evident Doppler effect in KI atomic and CH molecular lines and have measured the displacement of diffuse bands by cross-correlation with the template spectrum from the survey by Galazutdinov et al. (2000) where measurements are based on a single-cloud object HD23180. However, in almost all cases the reddened OB stars are observed through more than one cloud; i.e. the high resolving power is of critical importance. In fact the DIB profiles are much broader than those of atomic/molecular lines and thus their shapes are quite resistant against the Doppler split and are not expected when the split is not observed in atomic or molecular features. Nevertheless, in a vast majority of cases we observe some ill-defined averages along the chosen sightlines which makes the determination of physical conditions, leading to the formation of DIB carriers very complex.

Diffuse bands' carriers are believed to be concentrated in neutral interstellar clouds which are revealed by KI 7699 Å line (Table 1) or the methylidyne (CH) features (Megier et al. 2005). The review by Galazutdinov et al. (2000) is based on the assumption that the correction of the wavelength scale to the rest-wavelength frame by means of either KI or CH lines provides also the correction of DIBs to their laboratory wavelengths. The assumption seems justified in a vast majority of cases (see, e.g. DIB surveys by Hobbs et al. (2008); Bondar (2012)), but some exceptions have already been reported. Other interstellar absorption lines cannot be used for this purpose; e.g. the H and K lines of CaII are apparently formed in numerous tiny, Doppler shifted clouds which are mostly ionized (Megier et al. 2009).

Krelowski & Greenberg (1999) observed for the first time that diffuse bands are red-shifted while related to the interstellar NaI lines in stars HD37020, HD37022, HD37023, HD37042, HD37061 belonging to the Ori OB1 association. The observed red-shift was found to be quite small (~ 0.1 Å) yet very evident in all studied directions. The extinction curves of lines of sight to Ori OB1 targets are extremely peculiar (see Figs. 4.8 and 4.9 in Fitzpatrick & Massa, 2007) as well as interstellar spectrum: very weak molecular and narrow diffuse bands while broader diffuse bands are well seen. The targets in Ori OB1 are characterized by relatively weak simple interstellar radicals CH, CN and narrow DIBs (with respect to the color excess) making study of the positional displacement very difficult. Interestingly, the weakening does not concern so called "broad" diffuse bands, e.g. at 5780 and 6284 Å. So far the observed DIB's red-shifts are reported only in the above mentioned stellar aggregate (Ori OB1). Likely the peculiar physical conditions due to e.g., strong UV-flux irradiation from the nearby very hot young stars, do cause the observed displacement of diffuse bands.

The first object where some DIBs were reported as blue-shifted in relation to either KI or CH lines is HD34078 (Galazutdinov et al. 2006). The paper also demonstrated that the profiles of blue-shifted DIBs are broader than those observed in the spectrum of HD23180 used for comparison. The widths of the narrow DIB profiles seemingly grow towards blue. This moves the centers of these features to the same direction (Fig. 1) contributing to the net blue-shift effect.

According to Herbig (1999) the radial velocity of the CH 4300 Å lines observed in HD34078 has changed between 1949 and 1999 from 13.6 to 15.3 km/s. This may coincide with the variable intensity of this feature postulated by Rollinde et al. (2003). However, our current measurement (15.4 km/s) coincides with the 1999's value. It may suggest that the positional variability (if any) does not progress in the linear way.

The phenomenon of DIB blue-shifts is typical for the Sco OB1 association. Galazutdinov et al. (2008) reported the detection of blue-shifts for 20 diffuse bands, though some of the studied features are very weak and thus, the conclusions that concern them are uncertain.

In this paper we present a study of positional displacement and profile changes of diffuse bands in spectra of 4 objects (Tab.2, 3) including the previously studied HD34078 (Galazutdinov et al., 2006) and HD152233 (Galazutdinov et al., 2008) but using another instrument. We also observed two heavily reddened but apparently free of Doppler split effect objects HD73882 and HD169454. We confirm the earlier results and extend the number of studied diffuse bands using another instrument (Magellan/Mike), now with much higher signal-to-noise ratio of the carried out spectra. Thus, we confirm blue-shifts of many diffuse bands in the spectrum of HD152323 as well as our former detections for HD34078. HD73882 and HD169454 in general do not reveal noticeable displacements of diffuse bands.

2. Observational material

The spectra of HD34078 (AE Aur) and HD152233 (a member of Sco OB1 association) were recorded together with those of HD73882 and HD169454 with the aid of the Magellan/Clay telescope at the Las Campanas Observatory in Chile using the MIKE spectrograph (Bernstein et al. 2003) with a 0.35×5 arcs slit. The recorded spectra are averages (in the pixel space) of 19 – 60 individual exposures to achieve a high S/N ratio. We estimated the resolving power using the solitary Thorium lines. It is $\sim 56,000$ ($\Delta\lambda \sim 5.4 \text{ km s}^{-1}$) on the blue branch (3600-5000 Å) and $\sim 77,000$ ($\Delta\lambda \sim 3.9 \text{ km s}^{-1}$) on the red branch (4800-9400 Å). In all cases we used HD116658 (Spica) as a telluric line divisor.

General information about observed lines of sight is given in Table 2, including the column density of neutral atomic and molecular hydrogen. The spectra were processed and measured in a standard way using both IRAF (Tody 1986) and our own DECH¹ codes.

2.1. The wavelength calibration

The wavelength scale of the studied spectra was calculated on the basis of a global polynomial equation:

$$\lambda(x, m) = \sum_{i=0}^k \sum_{j=0}^n a_{ij} x^i m^j \quad (1)$$

where a_{ij} are polynomial coefficients; x - the pixel position in the direction of dispersion; m - the order number. The final solution uses typically 300-1200 lines of Thorium (depending on the spectrograph's arm) and the rms residual error between the fit and the position of the lines is usually $\leq 0.003 \text{ Å}$, i.e. much lower than 1 km s^{-1} .

Prior to the measurements of displacement of diffuse bands, the wavelength scale of all spectra was shifted to move the CH 4300 Å line to their laboratory positions, i.e. the rest wavelength velocity frame was set interstellar. Thereto, the wavelength correction in Angstroms was calculated for each pixel of the spectrum based on the measured CH 4300 shift in the radial velocity (km s^{-1}) scale.

The selection of CH as a rest point is argued by the fact that in most of surveys the radial velocity of the cores of profiles of CH 4300 and KI 7699 are almost identical. Moreover, ultra-high resolution profiles of CH 4300 and KI 7699 in spectra of HD23180 studied by Crane, Lambert & Sheffer (1995) and Welty & Hobbs (2001) report the radial velocity values of the cores of features as $+14.6$ and $+13.5 \text{ km s}^{-1}$ respectively, i.e. the wavelength uncertainty does not exceed 0.01 Å .

¹<http://gazinur.com/DECH-software.html>

2.2. Full width at the half of the maximum (FWHM) of the diffuse bands

Width of diffuse bands cannot be precisely measured by Gaussian or Voigt fit because of irregular shape of profiles. To measure the FWHM, the studied profiles were smoothed by a Fourier filter. Then, the minimum of the smoothed curve is found as well as two required points of the smooth curve at the half-intensity. The method was well illustrated by Bondar (2012) in his figure 3 with a difference that Bondar used a Chebyshev polynomial fit instead of our Fourier smoothing applied.

2.3. Measurements of displacement

To minimize the effects of uncertain rest wavelengths we measured the displacement of diffuse bands by the cross-correlation of profiles of diffuse bands in the studied objects with those of the well-studied line of sight HD23180 - an object with the negligible Doppler split. *Id est*, diffuse bands profiles of each studied spectrum were cross-correlated with the corresponding profiles of the template. Then, the measured displacement was applied to the rest wavelength of the studied diffuse band. We might note again, that these rest wavelengths were determined as means of that particular object HD23180, see our survey Galazutdinov et al., 2000.

For most of diffuse bands we have used as a template the average spectrum of HD23180 from our survey (Galazutdinov et al. (2000)) and, in cases of weaker diffuse bands, we used more recent spectra of the same target from our database. Before the measurements, the template spectrum profiles were smoothed using the Fourier transform based filter. Measurements of profile displacements have been done using our DECH code procedure based on the algorithm developed by Tonry & Davis (1979) and Verschueren & David (1999).

Cross-correlation of two sufficiently symmetric (e.g., DIBs 5780 and 5850, see Fig. 2) profiles produces also symmetric Gaussian-like cross correlation function (CCF), where the position of the maximum is evident (Fig.3). However, most of the diffuse bands do not exhibit symmetric profiles (e.g. DIB 5797). Nevertheless, the close similarity of measured profiles with those of the template also produce sufficiently symmetric CCF with evident position of the maximum of the correlation.

Some diffuse bands are broad and shallow making their analysis rather difficult (e.g. DIB 5776): continuum normalization plays a crucial role in formation of the shape of subsequent cross-correlation functions (CCF), although does not affect much to the peak position, which can be estimated without a doubt.

DECH software continuum normalization method is based on the cubic spline interpolation *over* the manually set fiducial marks. As it was mentioned above, the continuum normalization plays a crucial role for the shape of the subsequent CCF. Even in complicated cases (e.g., noisy and weak DIB with irregular asymmetric profile) the resulting CCF enable the confident finding the top position, i.e. the value of displacement.

Results of measurements are presented in Tab. 3 and Fig.4.

3. Results

In the present survey we consider a sample of diffuse bands free of evident blending with stellar lines and being strong enough to provide sufficiently high S/N ratios inside their profiles. The four considered spectra were shifted to the rest wavelength velocity scale using the CH 4300 Å. In Fig. 5 CH 4300 Å line is shown together with CH B-X (0,0) and CN B-X (0,0) bands in the blue range. The spectra in the left panel of Fig. 5 are normalized to identical depths of the CH 3886 Å feature. It is evident that the position of the lines carried by simple interstellar radicals coincide in all targets in the frame of measurement uncertainties. This suggests that all possible displacements of interstellar features are likely caused by physical modifications of DIB profiles unless some clouds, not revealed by the depicted lines, are present along the sightlines. The relative (to CH) abundance of CN is much higher (by an order of magnitude) towards our comparison objects: HD73882 and HD169454 (see also Krelowski et al. 2012). This considerable difference in the relative abundances of simple interstellar radicals proves different physical/chemical conditions in the clouds situated along the sight lines to our targets.

In all our targets we can trace the $C_3 \tilde{A}^a \Pi_u - \tilde{X}^a \Sigma_g^+$ 000-000 band (Fig. 6). The point to be emphasized is that the rotational temperature of HD34078 of C_3 molecule is very high in contrast to HD169454 – see Fig. 6 confirming results of *Ádámkóvics et al. (2003)*. According to them T_{rot} equals 42K for HD169454 and 171K for HD34078. **Our recent result for C_3 T_{rot} is 21 ± 1 K.** T_{rot} observed towards our standard, HD23180 is 90K, i.e. resides between HD169454 and HD34078.

We have measured positional displacement, FWHM (full widths at the half maxima) and equivalent widths of 29 diffuse bands (Table 3 and Fig. 4). Our measurements confirm the blue-shifts of the DIBs reported by *Galazutdinov et al. (2006)* in the spectrum of HD34078. Similar effect is seen towards HD152223 (previously reported by *Galazutdinov et al. (2008)*) – some bands show even greater displacements than those in HD34078. Evidently these two targets show a ”blue-shift” of most of diffuse bands in general. Generally speaking, careful measurements reveal a common “instability” of positions of diffuse bands from object to object with amplitude within $\sim \pm 5 \text{ km s}^{-1}$.

The main DIBs (the first ever observed) near 5780 and 5797 Å are shown in Fig. 2 along with their weaker neighbors 5776 and 5850. Both DIB5797 and DIB5776 are evidently blue-shifted in the spectra of HD34078 and in HD152233 confirming the result of *Galazutdinov et al. (2008)*. The 5797 profile is substantially broadened in the spectrum of HD34078 in comparison to HD73882 but, the 5797 profile in HD152233, though also blue-shifted, is not broadened at all (Fig. 1). Evident broadening of many diffuse bands is well seen in the spectra of HD34078 (Fig.7a and 7b). Interestingly, in the case of HD152233 the evident blue shift seen in many diffuse bands (Fig. 4) is

not accompanied with the broadening of their profiles (Fig. 7a).

It is worth noting that one of the major diffuse bands, strong and broad DIB5780 exhibits **displacement** of the peak position: indeed, while the feature is slightly blue shifted in spectra of HD34078 and HD152233, the evident red-shift of the DIB is seen in the spectrum of HD169454 where the diffuse band is strongest in the sample. It may be interesting to reveal possible relation between the positional displacement and strength (i.e. reddening) of this band.

The notable positional displacement can be observed in the case of the narrow 6196 DIB (Galazutdinov et al. 2006, 2008). The variable profile of this DIB was related to the T_{rot} of the C_2 molecule by Kaźmierczak et al. (2009).

Let’s discuss finally the possible reasons for the observed wavelength shifts of diffuse bands using the most narrow and relatively deep DIB at 6196, demonstrating evident displacements. The estimates of its central wavelength are a bit floating (Table 1) from author to author, but in general they remain in the range of 0.05 Å. Fig.8 presents DIB6196 shown together with four identified interstellar lines: CH – 4300 Å, CH⁺ – 4232 Å, CaII – 3933 Å and KI – 7699 Å in the spectra of our targets in the scale of heliocentric radial velocities.

The comparison suggests the following conclusions:

- radial velocities of KI and CH lines are always very close
- the radial velocity of the 6196 DIB does not always agree with those of KI, CH and CH⁺
- the position of 6196 in HD34078 may coincide with a very weak Doppler component of KI, having no correspondence in profiles of molecular lines;
- in the case of HD152233 the DIB position coincides with weaker (but still strong) component of CH⁺ – this component is very weak in the CH profile, but present in CaII and NaI lines.

4. Discussion and Conclusions

The published conclusions of Galazutdinov et al. (2006, 2008) are now confirmed using an additional instrument from another observatory. Moreover we extended our considerations to the weaker DIBs which were out of reach while using spectra from the Terskol and Bohyunsan observatories. The average displacement of 29 measured diffuse bands relative to CH 4300 Å line is $+1.0 \pm 2.1$ km s⁻¹ for HD73882, $+0.8 \pm 2.9$ km s⁻¹ for HD169454, -4.0 ± 3.8 km s⁻¹ for HD34078 and -3.6 ± 3.1 km s⁻¹ for HD152233. However, just 18 out of measured 29 diffuse bands exhibit blue shift in both directions to HD152233 and HD34078. Two weak diffuse bands in blue range (DIBs 4985 and 5542) are blue-shifted in HD152233 only. Also, there are weak 3 bands (6117, 6140 and 6376) with measured blue-shift in HD34078 but not firmly confirmed in HD34078.

Our Fig.7 proves the general broadening of diffuse band in HD34078. However, the relation between the broadening magnitude and displacement is not revealed: see Fig. 7b.

The diffuse bands wavelength variations are thus proven beyond a doubt, though the origin of the shifts remains unclear. Our sample of targets is evidently too small to make a definite conclusion that DIB positions are related to the T_{rot} of e.g. simple carbon chains since such a conclusion would be based on three points only. HD34078 is a very peculiar object in which the C_3 rotational temperature is the highest ever observed (Ádámkóvics et al., 2003) but HD152233 seems to be very similar in this respect. Our standard, HD23180, represents an average T_{rot} and, usually, also an average DIB position. Temperature variations, acting more or less like in the profile of C_3 band but in species of lower rotational constants, may change the observed DIB profiles, shifting their centers to the blue and altering the substructure systems seen in DIB profiles (see e.g. Fig.11 in Motylewski et al. (2000)). The most abundant interstellar molecule H_2 was also proven to be at highly excited rotational states towards HD34078 (Boisse et al. 2005). Moreover, the CH abundance in its direction is twice as big as in average for such an E(B-V); HD152233 does not share this property. A variability of the CH and CH^+ abundance in HD34078 was already suggested by Boisse et al.(2009).

The observed interstellar features, seen in the spectra of HD34078 and HD152233 are evidently originating in specific environments and deserve more observation. However, the behavior of DIBs in both objects is not identical. As shown in Fig. 2 one of main DIBs (5797) is blue-shifted in the spectra of the above targets if compared to that of HD73882. However, if to normalize the 5797 DIB to the same depth and to remove the shift in HD152233 (for clarity), one can see that the profile shape of this feature is identical in the latter object and in HD73882. On the other hand the DIB profile in HD34078 is much broader and only its center of gravity moves a bit blue-ward. Thus what we observe in HD152233 may be just a result of the Doppler shift, if the DIB originates in the cloud revealed by the CH^+ component(see also how the 6196 DIB behaves in HD152233 (Fig. 8) while in HD34078 it likely follows very specific environmental conditions.

Thus, we can summarize the possible explanations of observed displacements of diffuse bands:

- the peculiar environmental conditions revealed by e.g. high rotational temperatures of simple molecules; a good example is HD34078 where we observe unusually high rotational temperatures of simple molecular species, such as C_2 , C_3 or CN. We believe that CH and CH^+ can be rotationally excited but our existing spectra show too low S/N ratio – insufficient for checking such subtle effects. We have already demonstrated (Galazutdinov et al. 1998) that DIBs can be observed when color excess is practically zero. One can expect such components in certain DIBs originated in peculiar conditions.
- simply due to Doppler effect, i.e. unresolved multiple Doppler components that cause the movement of the center of the broadened profile (see Fig. 8); but in this case one meets a cloud with peculiar chemical composition or unusual physical parameters, i.e the "shifted" diffuse band does not correspond to the main (deepest) CH or KI component (Fig. 8), i.e.

the diffuse band carrier(s) are situated somewhere apart from the main "body" of the cloud.

More definite result requires much more representative sample of detected DIB shifts though one important conclusion can be inferred: despite of good general correlation between diffuse bands and interstellar KI and CH (normally serving for "interstellar" wavelength scale correction), diffuse bands carriers may not be spatially correlated with simple atomic/molecular gas.

GG acknowledges the support of Chilean fund FONDECYT-regular (project 1120190). JK acknowledges the financial support of the Polish National Center for Science during the period 2012 - 2015 (grant UMO-2011/01/BST2/05399). GV acknowledges the support by the Russian Scientific Foundation (grant N 14-50-00043). We are grateful for the assistance of the Las Campanas observatory staff members.

REFERENCES

- Allen, M. M., 1994, *ApJ*, 424, 754
- Ádámkóvics, M., Blake, G. A. & McCall, B. J. 2003, *ApJ*, 595, 235
- Bernstein, R., Shectman, S. A., Gunnels, S. M., Mochnecki, S., Athey, A. E. 2003, *SPIE*, 4841, 1694
- Boissé, P., Le Petit, F., Rollinde, E. et al. 2005, *A&A*, 429, 509
- Boissé, P., Rollinde, E., Hily-Blant, P. et al. 2009, *A&A*, 501, 201
- Bondar, A., Kozak, M., Gnacinski, P., Galazutdinov, G. A., Beletsky, Y., Krelowski, J., 2007, *MNRAS*, 378, 893
- Bondar, A. 2012, *MNRAS*, 423, 725
- Crane, P., Lambert, D.L., Sheffer, Y., 1995, *ApJS*, 99, 107
- Fitzpatrick, E.L. & Massa, D. 2007, *ApJ*, 663, 320
- Galazutdinov, G.A. 1992, *Prep. Spets. Astrof. Obs.*, No 92
- Galazutdinov, G.A., Krelowski, J., Moutou, C., Musaev, F. A. 1998, *MNRAS* 295, 437
- Galazutdinov, G.A., Musaev, F. A., Krelowski, J., Walker, G. A. H. 2000, *PASP*, 112, 648
- Galazutdinov, G.A., Galazutdinov, G. A., Manico', G., Pirronello, V., Krelowski, J. 2004, *MNRAS*, 355, 169
- Galazutdinov, G.A., G. A., Manico, G., & Krelowski, J. 2006, *MNRAS*, 366, 1075

- Galazutdinov, G.A., LoCurto, G., Han Inwoo, Krelowski, J. 2008, PASP, 120, 178
- Galazutdinov, G.A., LoCurto, G., Krelowski, J. 2008, ApJ, 682, 1076
- Gudennavar, S.B., Bubbly, S.G., Preethi,K., Murthy,J., 2012, ApJ Sup.Ser., 199, 8
- Heger, M.L. 1922, Lick Obs. Bull. 10, 146
- Herbig, G.A.H. 1975, ApJ, 196, 129
- Herbig, G.A.H. & Soderblom, D.R. 1982, ApJ, 252, 610
- Herbig, G.A.H. 1999, PASP 111, 809
- Hobbs, L., York, D.G., Snow,T.P., Oka, T., Thorburn, J.A., Bishof, M., Friedman,S.D., McCall, B.J., Rachford, B., Sonnentrucker, P. and Welty, D.E., 2008, ApJ, 680, 1256
- Hobbs, L. M., York, D. G., Thorburn, J. A., Snow, T. P., Bishof, M., Friedman, S. D., McCall, B. J., Oka, T., Rachford, B., Sonnentrucker, P. and Welty, D. E., 2009, ApJ, 705, 32
- Kaźmierczak, M., Gnaciński, P., Schmidt, M.R., Galazutdinov, G.A., Bondar, A. & Krelowski, J. 2009, A&A, 498, 785
- Kerr et al. 1998, ApJ, 495, 941
- Krelowski, J., Galazutdinov, G. & Musaev, F.A. 1998, ApJ, 493, 217
- Krelowski, J., & Greenberg, J. M. 1999, A&A, 346, 199
- Krelowski, J., Galazutdinov, G. & Gnaciński, P. 2012, AN, 333, 627
- McCall, B.J., Griffin, R.E. 2013, Proc. R. Soc. A2013 469: 20120604
- Megier, A., Strobel, A., Bondar, A., Musaev, F. A., Han, , Inwoo, , Krelowski, J., & Galazutdinov, G. A. 2005, ApJ, 634, 451
- Megier, A., Strobel, A., Galazutdinov, G. A. & Krelowski, J. 2009, A&A, 507, 833
- Motylewski, T., Linnartz, H., Vaizert, O., Maier, J. P., Galazutdinov, G. A., Musaev, F. A., Krelowski, J., Walker, G. A. H., Bohlender, D. A., 2000, ApJ, 531, 312
- Porceddu, I., Benvenuti, P., Krelowski, J. 1991 A&A, 248, 188
- Rollinde, E., Boisse, P., Federman, S. R. & Pan, K. 2003, A&A 401, 215
- Sarre, P. J., Miles, J. R., Kerr, T. H., Hibbins, R. E., Fossey, S. J., Somerville, W. B. 1995, MNRAS, 277, 41
- Schmidt, M. R., Krelowski, J., Galazutdinov, G. A., Zhao, D., Haddad, M. A., Ubachs, W., Linnartz, H., 2014, MNRAS, 441, 1134

- Sonnentrucker, P., Welty, D. E., Thorburn, J. A., York, D. G., 2007, ApJS, 168, 58
- Thorburn, J. A., Hobbs, L. M., McCall, B. J., Oka, T., Welty, D. E., Friedman, S. D., Snow, T. P., Sonnentrucker, P., York, D. G. 2003, ApJ, 584, 339
- Tody, D. 1986, "The IRAF Data Reduction and Analysis System" in Proc. SPIE, Instrumentation in Astronomy VI, ed. D.L. Crawford, 627, 733
- Tonry, J., Davis, M., 1979, AJ, 84, 1511
- 2000, A&AS 142, 225
- Welty, D.L., Hobbs, L.M., 2001, ApJS, 133, 345
- Weselak, T., Schmidt, M. & Krelowski, J. 2000, A&AS 142, 239
- Weselak, T., Galazutdinov, G. A., Han, Inwoo, Krelowski, J. 2010, MNRAS, 401, 1308
- Verschueren, W., David, M., 1999, A&A Sup. Ser., 136, 591
- Westerlund, B. E., Krelowski, J. 1988, A&A, 203, 134

Table 1: Comparison of the rest wavelength of diffuse bands at 6196 and 6614 Å in different surveys. "Line" marks the features used to move the spectra to the rest wavelength frame.

Survey	line	DIB 6196	DIB 6614
Galazutdinov et al. (2000)	KI 7699	6195.97	6613.56
Weselak et al. (2000)	NaI D ₁ , D ₂	6196.05	6613.52
Hobbs et al. (2008)	KI 7699	6195.98	6613.62
Hobbs et al. (2009)	KI 7699	6196.09	6613.70
Bondar (2012)	CH 4300	6195.95	6613.58

Table 2: Observed targets. Column densities of molecular and neutral hydrogen are from Gudennavar et al. (2012) Rotational temperature for C₃ and C₂ molecules (lower transitions) are taken from: a - Ádámkovics et al. (2003); b - Schmidt et al. (2014); c - Sonnentrucker et al. (2007) .

HD	V	Sp/L	E(B-V)	N(H I) × 10 ²¹	N(H ₂) × 10 ²⁰	H ₂ fraction	C ₃ T _{rot} (K)	C ₂ T _{rot} (K) ^a
34078	6.0	O9.5V	0.53	1.5849 ^{+0.4568} _{-0.3546}	7.5858	0.32	171 ^a	120±10 ^a
73882	7.3	O9III	0.70	1.2882	12.882 ^{+2.6057} _{-2.1673}	0.5		23±5 ^c
152233	6.6	O6III:(f)p	0.45	1.9498	1.9498	0.1		
169454	6.7	O+...	1.12	0.08912	14.454	0.94	21±1 ^b	50±10 ^a

Table 3: The measured equivalent widths (EW in mÅ), positional displacement (km^0s^{-1}) relative to CH 4300, and full-width at the half-maximum (RV and FWHM in km s^{-1}) of the interstellar features relative to the rest wavelength position of CH 4300.313 Å line. Wavelength data source: g - Galazutdinov et al. (2000) measured in HD23180; h - Hobbs (2008) measured in HD204827. The last column exhibits the displacement span (in km s^{-1}).

	HD73882			HD169454			HD34078			HD152233			span
	RV	EW	FWHM	RV	EW	FWHM	RV	EW	FWHM	RV	EW	FWHM	
FeI 3859.9114	-3.6±0.1	3.9±0.4	15±3	-1.1±0.5	5.0±1.5	10±5	+0.2±0.2	6.4±0.1	8.9±0.2	-2.0±0.1	3.0±0.2	9.0±0.3	3.8
CN 3873.994	+0.3±0.1	19.8±0.2	6.1±0.2	-0.1±0.2	16.7±0.2	5.6±0.2	-0.7±0.5	2.9±0.4	8.1±0.1	+0.5±0.2	0.5±0.2	6.0±1.0	1.2
CN 3874.602	+0.3±0.1	34.6±0.3	6.3±0.2	-0.2±0.2	23.3±0.3	5.8±0.2	-0.6±0.2	9.0±2.0	8.5±0.5	-0.3±0.1	1.7±0.3	6.8±0.2	0.9
CN 3875.759	+0.4±0.1	12.0±0.3	6.0±0.2	-0.2±0.1	11.5±0.2	5.6±0.2	-1.5±0.7	1.5±1.0	9.1±0.2	+0.1±0.3	0.3±0.2	6.5±0.5	1.9
CH 3886.409	+0.0±0.1	7.7±0.3	7.8±0.5	-0.4±0.2	7.9±0.4	6.5±0.1	-0.6±0.1	19.5±1.0	8.9±0.2	-0.3±0.1	3.4±0.2	8.4±0.3	0.6
CH 3890.217	+0.0±0.1	5.7±0.3	7.3±0.5	-0.5±0.2	5.6±0.4	6.5±0.1	-0.6±0.5	10.9±0.7	9.1±0.2	-0.2±0.1	2.0±0.2	8.2±0.2	0.6
CaI 4226.728	-4.9±0.1	57.5±0.5	7.1±0.2	+0.5±0.3	16.3±0.9	10.5±0.3	+3.0±1.0	6.9±0.6	14.5±0.5	+0.0±0.2	7.6±0.4	6.6±0.1	7.9
CH+ 4232.548	-0.2±0.1	18.4±0.4	8.1±0.1	-0.8±0.3	17.9±0.9	8.5±0.3	-0.2±0.2	38.3±0.5	8.5±0.2	-0.8±0.2	21.6±0.2	14.0±0.1	0.6
CH 4300.313	+0.0±0.1	24.6±0.3	6.5±0.1	+0.0±0.1	28.5±0.5	6.4±0.2	+0.0±0.1	50.1±0.5	7.8±0.1	+0.0±0.1	12.8±0.2	6.9±0.1	0.0
KI 7698.965	-0.4±0.2	48.0±0.8	8.7±0.3	-0.4±0.2	211±1.0	8.1±0.2	+0.0±0.1	171.0±2.0	9.1±0.3	+0.0±0.1	127.0±1.0	6.7±0.2	0.4
DIB4726.33g	+0.6±2.3	56.0±9.9	190±9	-0.9±4.3	140.0±5.0	180±50	+0.1±1.5	99.3±9.9	190±5	-1.8±3.5	67.0±5.0	190±5	2.4
DIB4734.79h	+5.5±2.0	1.9±0.4	20±5	+2.5±1.0	6.2±1.0	31±5	+4.5±1.5	14.3±4.0	42±2	+3.0±2.1	4.2±0.6	26±3	3
DIB4762.52g	-2.0±2.4	43.5±4.0	140±5	-1.0±3.0	115.0±15	145±10	-5.5±1.6	93.5±9.0	135±10	-12.0±3.0	50.0±9.0	140±20	11
DIB4963.85g	-1.5±0.5	9.2±1.5	43±3	-2.0±1.0	26.3±1.2	41±2	-4.4±1.6	20.0±2.0	48±1	-3.6±0.3	12.4±0.6	39±1	2.9
DIB4984.77g	-2.5±3.5	4.9±1.3	35±2	-5.5±1.0	14.1±1.3	31±1	-9.5±2.0	7.9±1.0	37±1	-6.0±4.5	6.0±0.4	31±2	7
DIB5494.07g	+1.0±2.0	9.6±1.5	37±5	-1.2±0.2	23.4±1.6	31±2	-6.0±1.0	10.2±1.2	31±4	-6.0±1.0	12.8±1.2	35±2	7
DIB5512.65g	+0.0±2.0	2.0±1.0	34±3	-0.2±0.2	15.3±1.3	31±1	-1.2±0.4	6.6±1.0	46±3	-1.5±1.3	6.7±0.8	32±1	1.5
DIB5541.74g	-1.5±0.7	2.2±1.2	39±4	+1.3±0.4	8.5±1.0	32±2	+1.2±2.0	6.2±0.8	35±3	-1.5±0.5	5.2±0.9	41±1	2.8
DIB5544.95g	+0.0±2.0	6.4±1.0	47±2	+3.0±2.0	25.7±1.2	44±2	-6.3±2.2	3.8±0.6	46±3	-3.4±0.5	8.9±1.5	44±2	9.3
DIB5546.46g	-0.3±0.5	0.8±0.5	23±2	-4.0±2.0	7.3±1.5	30±3	-4.5±1.0	1.3±0.5	22±5	-3.5±1.7	3.4±0.5	31±4	4.2
DIB5775.89g	+0.5±1.0	5.7±1.1	50±5	+2.0±0.7	13.0±2.0	58±2	-9.5±3.0	7.0±2.0	43±1	-3.5±2.0	5.0±1.3	62±5	11.5
DIB5780.37g	+7.5±0.5	145.0±5.0	106±5	+8.0±1.0	467.0±5.0	110±1	+2.5±1.0	165.0±5.0	110±1	-1.7±0.3	215.0±3.0	105±1	9.7
DIB5796.99g	+0.5±1.8	34.0±1.4	40±3	+4.0±0.8	161.0±1.8	44±1	-4.3±1.4	56.0±1.5	51±2	-2.0±1.3	60.0±2.8	43±1	8.3
DIB5849.82g	-1.3±0.9	14.7±1.8	50±2	+0.7±0.1	68.6±1.8	42±1	-2.0±1.8	31.0±1.5	60±4	-3.0±0.5	28.0±2.0	45±1	3.7
DIB6065.31g	+3.3±3.0	2.5±0.5	30±7	+4.2±1.0	9.8±0.5	29±3	-0.9±0.3	6.8±1.0	30±3	-0.9±0.3	2.5±0.4	27±1	5.1
DIB6089.78g	+0.5±2.0	4.1±0.6	30±3	+0.7±0.6	26.3±0.6	28±1	-7.0±1.0	4.2±0.6	30±3	-2.0±1.0	6.6±0.5	28±2	7.7
DIB6108.05g	+1.3±2.0	2.5±0.5	20±3	+0.0±0.5	8.8±0.8	24±3	-6.0±4.0	4.6±0.9	36±3	-6.9±0.3	3.4±0.3	26±1	8.2
DIB6113.20g	+0.5±0.7	6.9±0.6	55±9	-0.5±1.0	18.5±1.7	34±3	+0.5±1.0	9.5±0.7	60±4	-2.5±2.7	14.0±1.3	48±1	3
DIB6116.84h	+1.3±0.3	5.0±1.5		-2.0±4.0	13.8±1.4	44±1	-12.5±2.5	9.6±1.1	64±2	-0.1±1.5	5.6±1.0		13.8
DIB6139.94g	-0.3±1.5	4.0±1.0	25±2	+0.0±0.7	13.0±1.0	28±3	-6.0±1.0	3.5±1.1	37±2	-0.5±1.0	6.0±1.0	60±30	6
DIB6161.84g	+0.7±1.0	1.2±0.5	30±9	+2.8±1.0	8.2±0.5	21±2	-2.7±1.0	2.5±0.8	30±5	-5.6±1.0	3.5±1.0	21±5	8.4
DIB6195.97g	+3.7±0.5	16.6±0.5	23±3	+1.8±0.2	62.0±1.0	24±2	-6.0±0.5	22.0±1.0	26±5	-5.6±0.2	24.0±1.0	24±3	9.7
DIB6203.08g	+0.5±1.0	29.6±1.5	63±1	+1.8±1.0	82.8±3.0	59±1	-5.2±3.0	37.0±1.5	69±1	-9.5±1.0	50.0±1.5	67±2	11.3
DIB6269.75g	+1.5±2.0	33.5±3.5	57±2	+1.7±0.5	104.0±5.8	57±2	-3.5±1.0	64.4±3.9	67±3	-7.2±0.5	44.5±5.0	60±4	8.9
DIB6283.85g	+1.1±0.5		187±9	+7.3±5.0		173±3	-1.4±3.0			-0.7±1.9		170±3	8.7
DIB6375.98g	+0.0±1.5	10.2±1.5		+2.0±2.0	51.0±3.5	38±4	-4.0±2.5	15.0±1.7	66±5	-1.0±1.5	23.2±2.2	55±5	6
DIB6379.32h	+3.1±0.2	12.3±0.7	31±2	+0.3±0.1	93.6±3.0	28±1	-6.0±0.9	188.0±2.0	35±3	-2.7±0.2	24.6±1.7	29±2	9.1
DIB6613.56g	+2.0±1.0	46.0±1.1	47±1	-0.5±0.5	192.0±3.0	45±1	-5.0±1.5	63.0±2.0	55±2	-5.0±0.5	82.0±2.0	46±2	7
DIB6660.64g	+2.0±0.5	5.7±0.7	29±1	-2.3±0.3	34.4±0.9	26±2	-8.5±1.0	6.0±2.0	28±5	-7.0±1.5	11.7±1.4	27±3	10.5

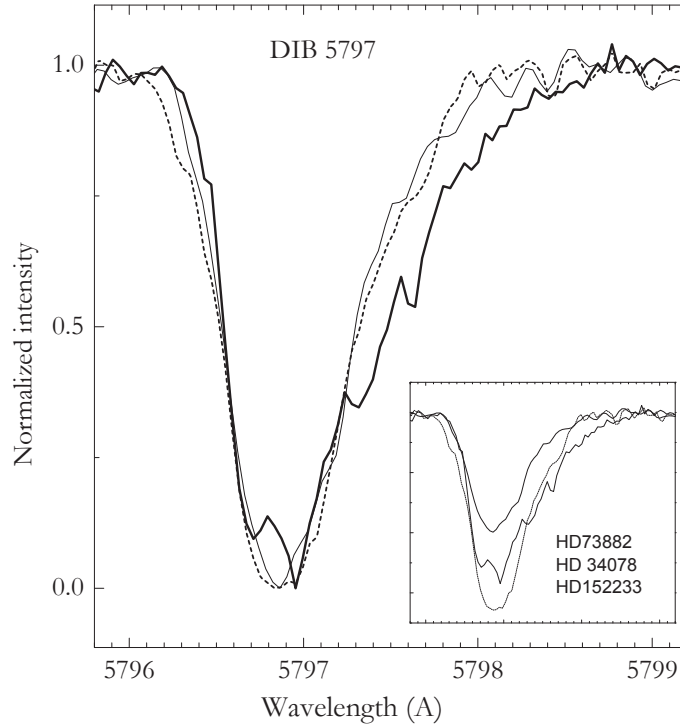


Fig. 1.— Profile of DIB 5797 in spectra of 3 program stars normalized to the same depth. Original profiles are shown in the small panel. The absolute wavelength scale is arbitrary – all profiles are shifted for more evident comparison of profiles. Thick solid line - HD34078, thin solid line - HD73882, dash line - HD152233. FWHM of the feature is almost identical in HD152233 and HD73882, i.e. the blue shift observed in HD152233 may suggest a Doppler origin while that of HD34078 can be due to the profile broadening.

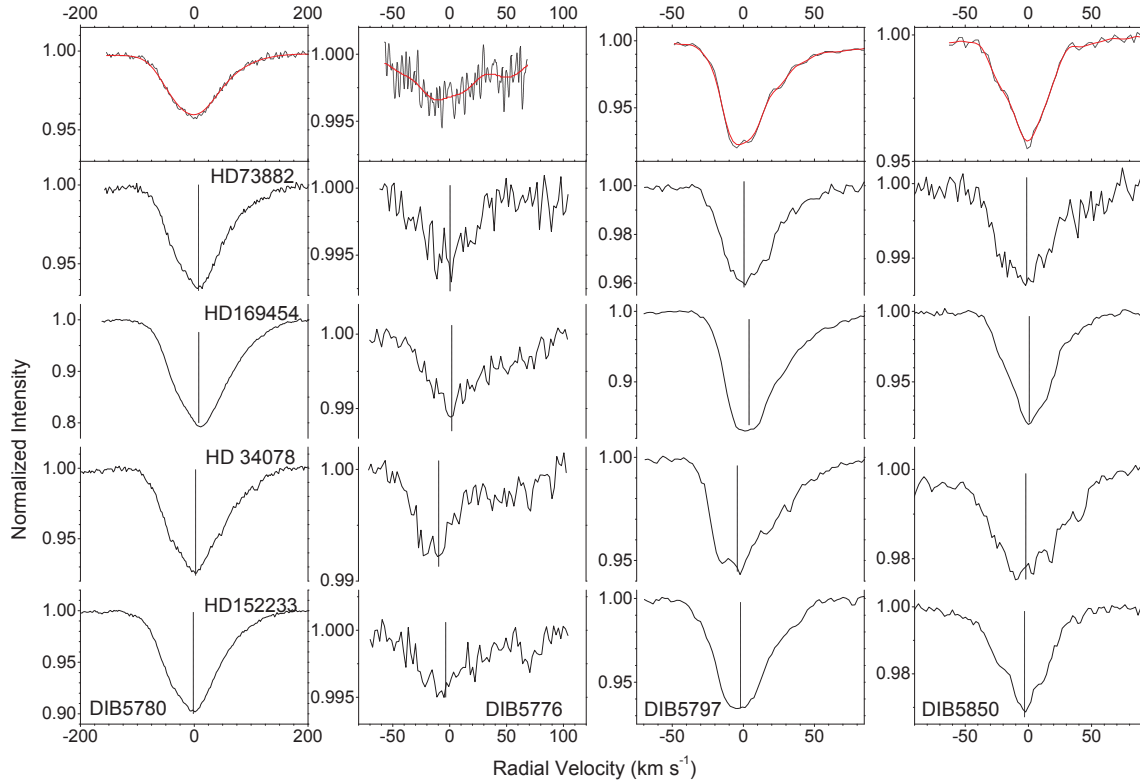


Fig. 2.— A sample of diffuse bands in studied spectra (bottom) shown together with a template spectrum (top). The template spectrum (the upper panels) is shown in its original form (black dash line) and as the Fourier-smoothed profiles (red solid lines). The latter were cross-correlated with studied DIBs for measurement the positional displacement. The vertical lines correspond to the measured shift position. (A color version of this figure is available in the online journal.)

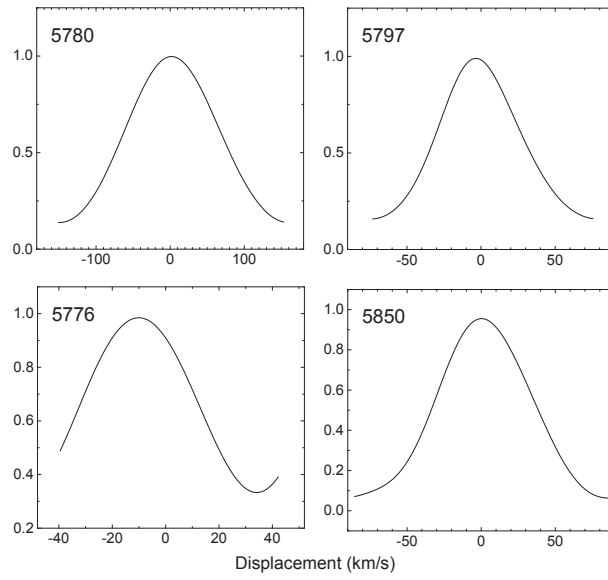


Fig. 3.— Cross-correlation functions of HD34078 diffuse bands shown in Fig. 6.

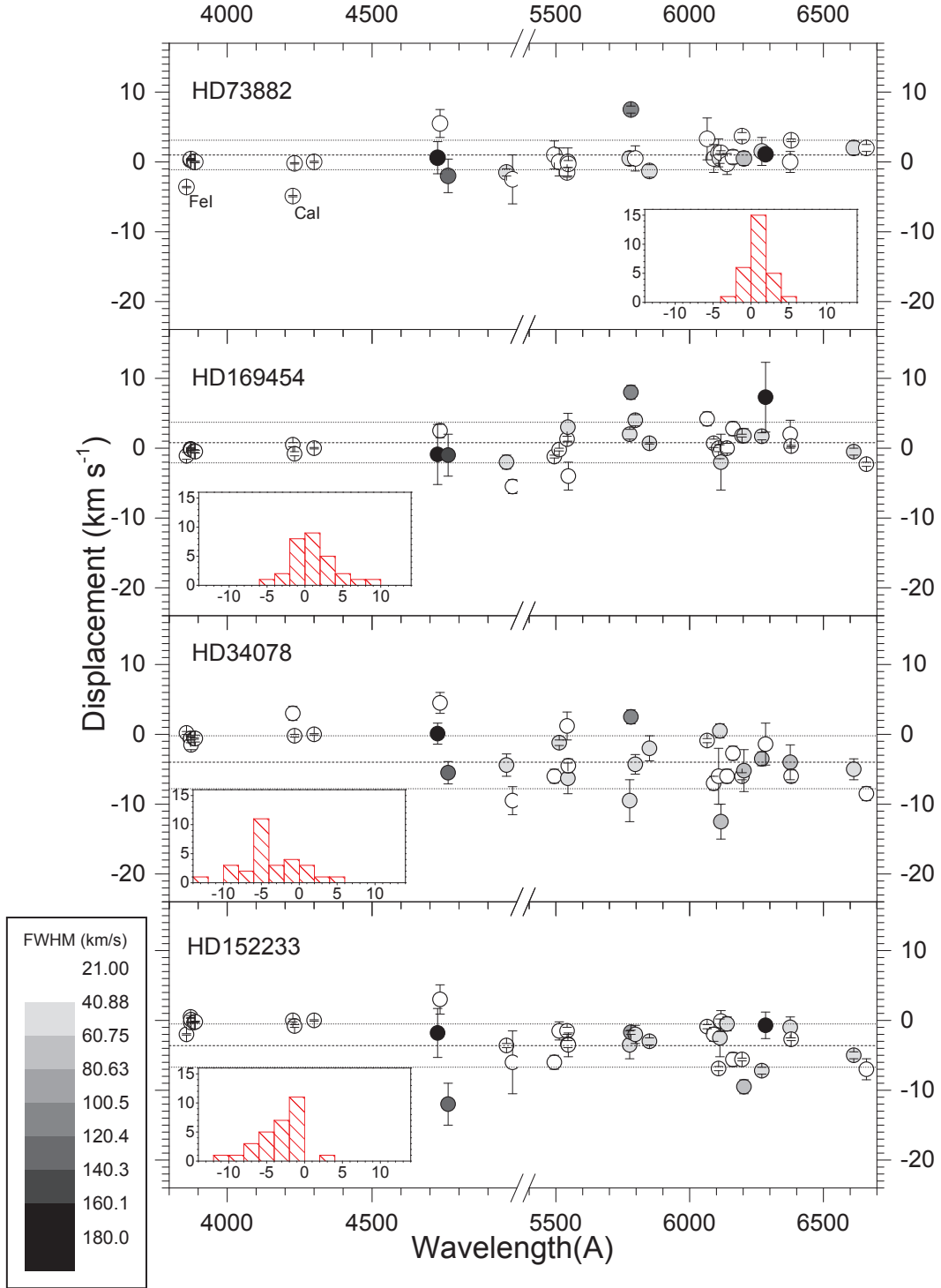


Fig. 4.— Positional displacement of interstellar features relative to the CH 4300 Å band (see Tab. 3) and histograms of the distribution of displacements (for DIBs only) for each studied object. Points with the wavelength lower than 4500 Å are well known molecules and atoms. Note the displaced FeI and CaI revealing tiny CaFe clouds (Bondar et al., 2007). Dash and dot lines represent the mean displacement and limits of the standard deviation for diffuse bands only.

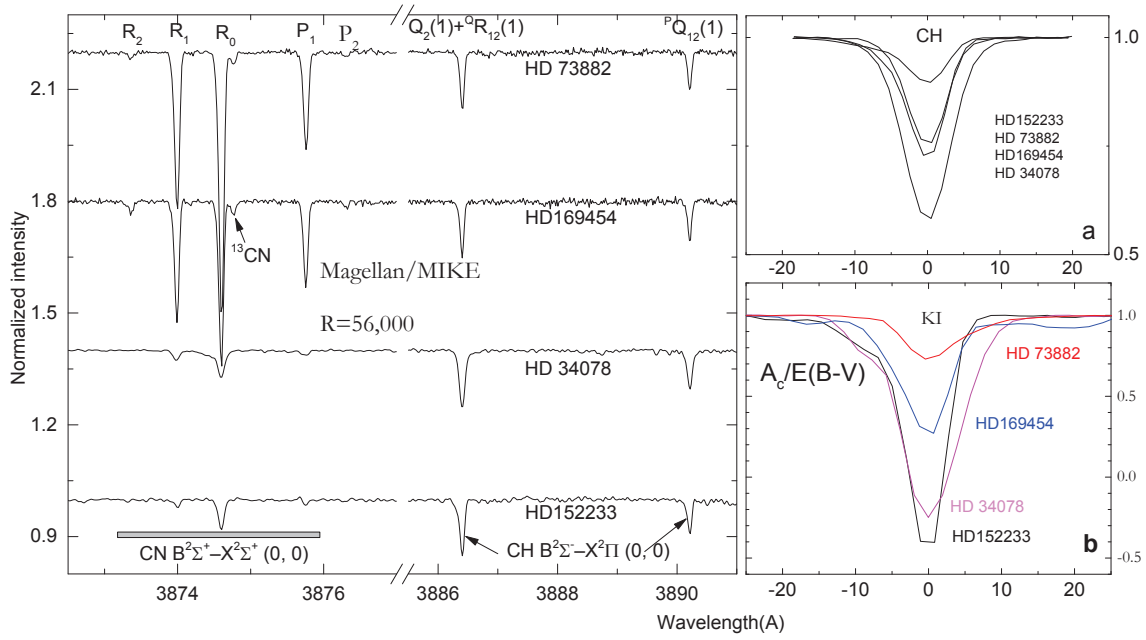


Fig. 5.— **Left.** CN and CH B-X (0,0) violet interstellar bands. The features have been shifted to the rest wavelength velocity frame together with the whole spectra. The spectra are normalized to the identical depth of the CH 3886 Å feature. **Right. a** CH 4300 Å line profiles in spectra of observed targets. Note the lack of Doppler split. **Right. b** The potassium $\lambda 7699$ Å line, normalized to E(B-V) in the spectra of our targets. Apparently the ionization level of potassium is much lower in HD34078 and in HD152233 than in the two remaining targets. Note the lack of Doppler split.

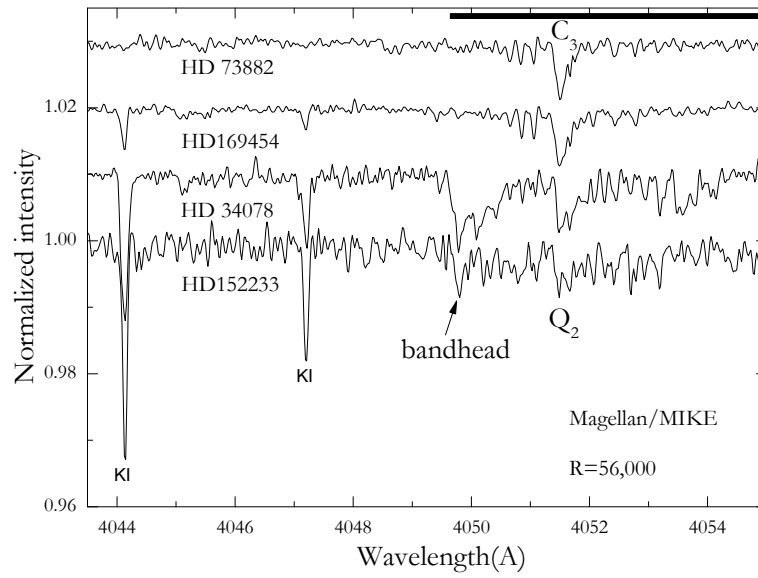


Fig. 6.— The $C_3 \tilde{A}^a \Pi_u - \tilde{X}^a \Sigma_g^+ 000-000$ band observed in all considered targets. Note the very strong bandheads in HD34078 and HD152233 which demonstrate very high rotational temperatures.

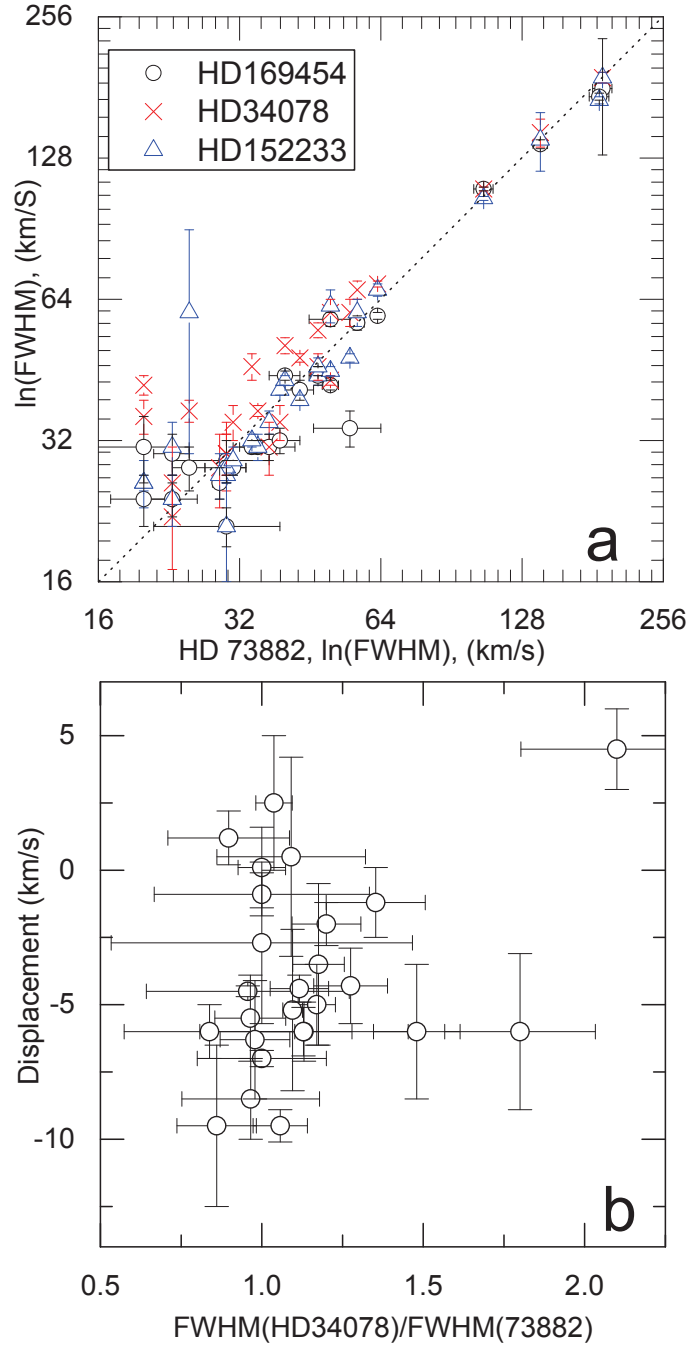


Fig. 7.— **a.** Comparison of the width of diffuse interstellar bands measured in program stars. **b.** The ratio of $\text{FWHM}(\text{HD}34078)/\text{FWHM}(\text{HD}73882)$ versus the shift. Note the lack of correlation.

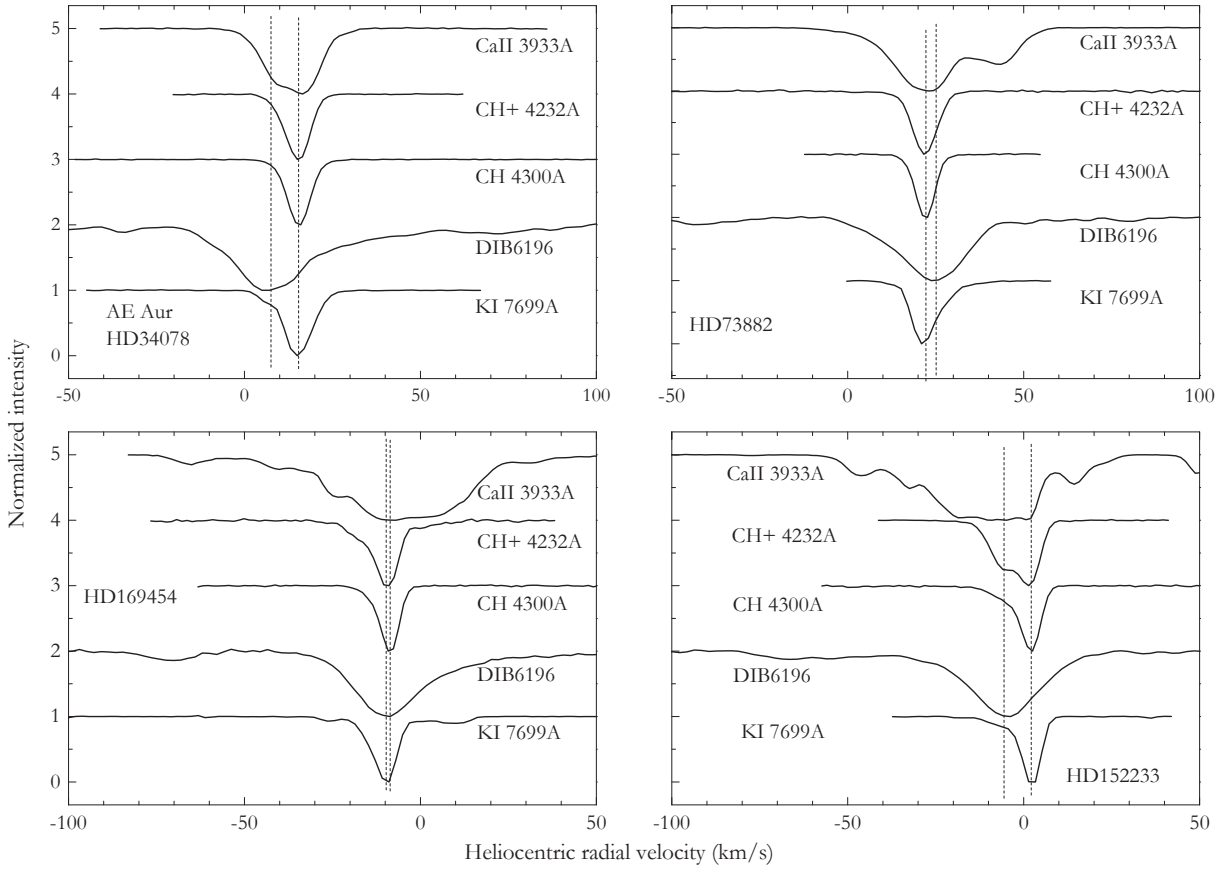


Fig. 8.— The identified interstellar features and the 6196 DIB plotted in the radial velocity scale in spectra of our targets. Vertical dotted lines mark position of CH 4300 and DIB6196.